Imaging methods in random scattering media

Akira Ishimaru, #Sermsak Jaruwatanadilok, and Yasuo Kuga
Department of Electrical Engineering, University of Washington, Seattle, WA, 98195 USA
sermsak@u.washington.edu

1. Introduction

In this paper, we present an analysis and comparison of several imaging methods of point targets in random scattering media. We derive the multi-static matrix and time-reversal matrix based on the mutual coherence function [1]. This includes the interactions of the random scattering media with the targets of interest, which captures the effect of random media to the imaging of the targets. Several imaging modalities including time-reversal (TR) [2], time-reversal Multiple Signal Classification (TR-MUSIC) [3], Synthetic Aperture Radar (SAR), minimum variance beam forming (or Capon's method), and modified beam forming (related to coherent tomographic array imaging) are applied to produce images and their performances are compared. We also investigate the effects of the random media characteristics on the images.

2. Received signal model, multi-static matrix and time-reversal matrix

The geometry of the problem is sketched in Fig. 1. The transmitting and received array of size N is used. There are M targets located in the imaging domain. A strip of random scattering medium of length d_2 starts at a distance d_1 from the array. The random scattering medium is characterized by optical depth, scattering and absorption coefficient and anisotropy factor.

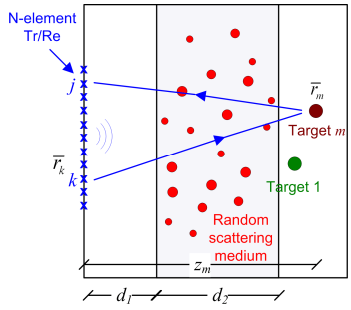

Fig. 1: Geometry of the problem

The array transmits a wave, which could be continuous or pulse. Then, the wave encounters absorption and scattering from the random scattering medium and reflection from the targets. The scattered wave is then detected at the receiving antenna array. From the received signal, we can form a multi-static data matrix $\mathbf{K}$ of size $N \times N$ given by

$$\mathbf{K} = \sum_{m=1}^{M} \tau_m \mathbf{g}_m \tilde{\mathbf{g}}_m \tag{1}$$

where $\mathbf{g}_m = \left[G(\bar{r}_m, \bar{r}_1) \quad G(\bar{r}_m, \bar{r}_2) \quad \ldots \quad G(\bar{r}_m, \bar{r}_N) \right]^T$, $\tilde{\mathbf{g}}_m$ is a transpose of $\mathbf{g}_m$. $G(\bar{r}_m, \bar{r}_k)$ is the stochastic Green's function where the observation point is $\bar{r}_m$ and the source is at $\bar{r}_k$. The reflectivity of the m^{th} target is denoted by τ_m. The 'time-reversal matrix' is given by

$$\mathbf{T} = \tilde{\mathbf{K}}^* \mathbf{K} = \sum_{m'=1}^{M} \sum_{m=1}^{M} \tau_{m'}^* \tau_m \mathbf{g}_{m'}^* \tilde{\mathbf{g}}_{m'}^* \mathbf{g}_m \tilde{\mathbf{g}}_m \tag{2}$$

The symbol * denotes the conjugation. The $k'k$ element of the matrix $\mathbf{T}$ can be written as

$$T_{k'k} = \sum_{m=1}^{M}\sum_{m'=1}^{M} \tau_{m'}^{*}\tau_{m} \sum_{j=1}^{N} \Gamma_{k'k}(m',m) \tag{3}$$

where the mutual coherence function $\Gamma_{k'k}$ is given by

$$\Gamma_{k'k}(m',m) = \left\langle G_k G_{k'}^{*} G_j G_{j'}^{*} \right\rangle = G_{k'o}^{*}(m') G_{ko}(m) G_{j'o}^{*}(m') G_{jo}(m) Q \tag{4}$$

$$Q = \exp(-2\tau_o) + F_s \exp(-2\tau_o)\left(X_{kk'} + X_{jj'} + X_{jk'} + X_{kj'}\right) + F_s^2\left(X_{kk'}X_{jj'} + X_{jk'}X_{kj'}\right),$$

$$\tau_s = \int_{d_1}^{d_1+d_2} b\,dz = b d_2,\ \tau_o = \int_{d_1}^{d_1+d_2} (a+b)\,dz = (a+b)d_2,\ \ \tau_o = \tau_s + \tau_a,\ F_s = 1-\exp(-\tau_s),$$

$$X_{ij} = \exp\left(-\tau_a - \frac{\left|\overline{\rho}_i - \overline{\rho}_j\right|^2}{\rho_o^2}\right);\ \ \overline{\rho}_i = \sqrt{\overline{x}_i^2 + \overline{y}_i^2};\ \ \frac{1}{\rho_o^2} = \frac{\tau_s k^2\left[(d_1+d_2)^3 - d_1^3\right]}{12\alpha_p L^2 d_2 F_s}.$$

The factor Q represents the contribution from the random scattering medium. The characteristics of the medium are captured in the parameter a and b where a is the absorption coefficient and b is the scattering coefficient. The quantities ρ_o and α_p are the coherence length and the anisotropy parameter, respectively. The functions G's are free-space Green's function given in parabolic approximation form by

$$\begin{aligned} G_{ko}(m) &= \frac{1}{4\pi L}\exp\left[ik\left(z_m + \frac{\left|\overline{\rho}_m - \overline{\rho}_k\right|^2}{2z_m}\right)\right];\ G_{k'o}^{*}(m') = \frac{1}{4\pi L}\exp\left[-ik\left(z_{m'} + \frac{\left|\overline{\rho}'_m - \overline{\rho}'_k\right|^2}{2z'_m}\right)\right] \\ G_{jo}(m) &= \frac{1}{4\pi L}\exp\left[ik\left(z_m + \frac{\left|\overline{\rho}_m - \overline{\rho}_j\right|^2}{2z_m}\right)\right];\ G_{j'o}^{*}(m') = \frac{1}{4\pi L}\exp\left[-ik\left(z_{m'} + \frac{\left|\overline{\rho}'_m - \overline{\rho}'_j\right|^2}{2z'_m}\right)\right] \end{aligned} \tag{5}$$

The eigen analysis of the time-reversal matrix $\mathbf{T}$ is given by

$$\mathbf{T}\mathbf{v}_p = \lambda_p \mathbf{v}_p;\ \ \mathbf{v}_p = N \text{ eigenvectors},\ \lambda_p = N \text{ eigenvalue} \tag{6}$$

These will be used later in this paper.

3. Imaging methods

Several imaging methods are investigated. All methods uses a steering vector given by

$$\mathbf{g}_s = \begin{bmatrix} G_{s1} & \cdots & G_{sN} \end{bmatrix}^T \tag{7}$$

where the steering Green's function is given by $G_{si} = \frac{1}{4\pi L_s}\exp\left(ikL_s + ik\frac{\left|\overline{\rho}_s - \overline{\rho}_i\right|^2}{2L_s}\right)$ and $\overline{\rho}_s$ is the location of the steering point.

Time-Reversal MUSIC Imaging

Imaging by TR-MUSIC is done using the time-reversal matrix T and the steering vector $\mathbf{g}_s$ by

$$\psi_{TR-MUSIC} = \frac{1}{\sum_{p=M+1}^{N-1}\int d\omega U^2 \left|\mathbf{g}_s' \mathbf{v}_p\right|} \tag{8}$$

where $U = \left(2\sqrt{\pi}/\Delta\omega\right)\exp\left(-(\omega-\omega_o)^2/(\Delta\omega)^2\right)$; $k = \omega/c$, $\Delta\omega$ is the bandwidth, ω_o is the centre frequency and $\mathbf{g}_s'$ denotes conjugate transpose of $\mathbf{g}_s$.

Time-Reversal Imaging

$$\psi_{TR} = \int d\omega U^2 \lambda_1 \mathbf{g}_s' \mathbf{v}_1 \tag{9}$$

where $\mathbf{v}_1$ is the eigenvector corresponding to the largest eigenvalue

SAR Imaging

$$\psi_{SAR2} = \int d\omega |U|^4 \sum_i \sum_j \left\langle G_i^2 G_j^{*2} \right\rangle G_{si}^{*2} G_{sj}^2 \tag{10}$$

where $\left\langle G_i^2 G_j^{*2} \right\rangle = \left(G_{io} G_{jo}^*\right)^2 \left[2\left(\exp\left(-Q_{ij}\right)\right)^2 - \exp\left(-2\tau_o\right) \right] \triangleq \left(G_{io} G_{jo}^*\right)^2 R_{ij}$,

$$R_{ij} = 2\left(\exp\left(-\tau_o\right) + F_s \exp\left(-\tau_a - \frac{\left|\bar{\rho}_i - \bar{\rho}_j\right|^2}{\rho_o^2} \right) \right)^2 - \exp\left(-2\tau_o\right)$$

Modified Beam Forming

$$\psi_{MBF} = \int d\omega |U|^4 \sum_i \sum_j \sum_p \sum_q \left\langle G_i G_j G_p^* G_q^* \right\rangle \left(G_{si}^* G_{sj}^* G_{sp} G_{sq} \right) \tag{11}$$

Minimum Variance Beam Forming (Capon's method)

$$\psi_{Capon} = \frac{1}{\int\int d\omega |U|^4 \mathbf{g}_s' \mathbf{R}^{-1} \mathbf{g}_s} \tag{12}$$

where $\mathbf{R} = \mathbf{K}\mathbf{K}' + \sigma^2 \mathbf{I}$, the noise power is given by $\sigma^2 = \frac{Trace\left(\mathbf{K}\mathbf{K}'\right)}{SNR}$; $\mathbf{I}$ = identity matrix.

4. Results and Comparisons

The results of imaging in random scattering media are illustrated in Fig. 2. We use $\Delta\omega = 0.01$, $N = 41$, $L = 50\lambda$, OD = 1.0, and $d_1 = d_2 = 25\lambda$ in these calculations. The target is located at $(50\lambda, 50\lambda)$. Fig. 2 shows the geometry of the problem and its images from several methods discussed above. Time-reversal MUSIC provides the best resolution image. Fig. 3 compares the longitudinal and lateral resolutions for these methods as a function of the optical depth. As the optical depth increases, the resolution gets worse but at different rates.

Acknowledgments

This project is supported by the National Science Foundation under Grant ECS-0601394 and the Office of Naval Research under Grant N00014-07-1-0428.

References

[1] A. Ishimaru, S. Jaruwatanadilok, Y. Kuga, "Time reversal effects in random scattering media on superresolution, shower curtain effects, and backscattering enhancement," *Radio Science*, Vol. 42, pp. RS6S28, 2007.

[2] M. E. Yavuz and F. L. Teixeira, "Space-frequency ultrawideband time-reversal imaging," *IEEE Transactions on Geoscience and Remote Sensing*, Vol. 46, pp. 1115-24, 2008.

[3] A. J. Devaney, "Time reversal imaging of obscured targets from multistatic data," *IEEE Transactions on Antennas and Propagation*, Vol. 53, pp. 1600-10, 2005.

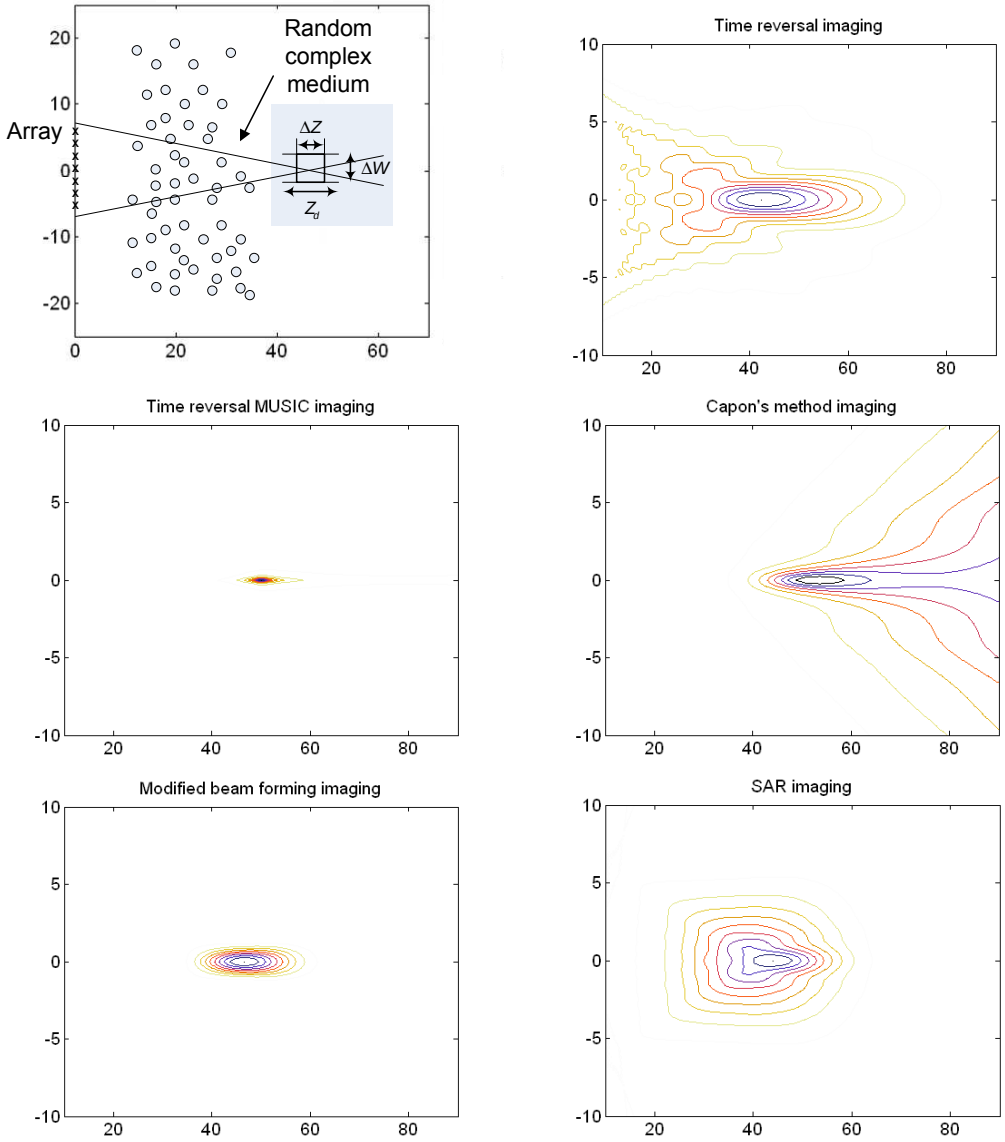

Fig. 2: Images of a single object in a random scattering medium using several imaging methods

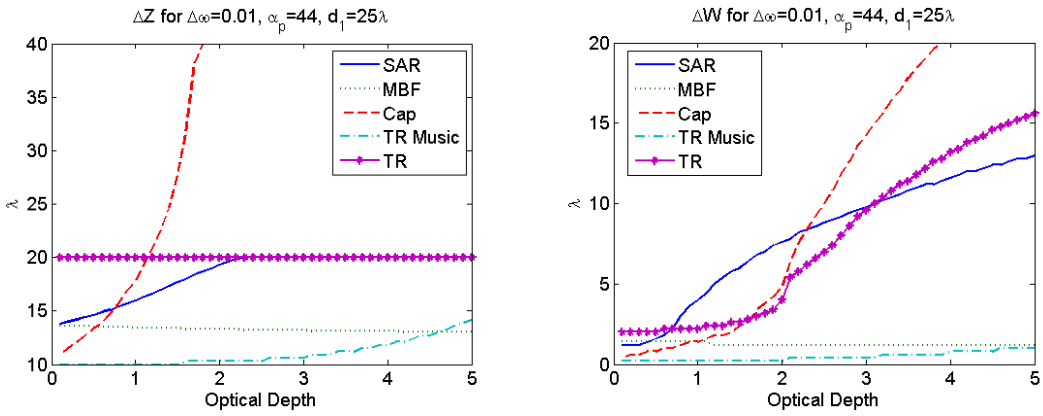

Fig. 3: Resolution comparison among imaging methods (a) longitudinal, and (b) lateral